Instituto Nacional de Investigación y Tecnología Agraria y Alimentaria (INIA)
Available online at www.inia.es/forestsystems
http://dx.doi.org/10.5424/fs/2013222-03477

Forest Systems 2013 22(2), 222-231
ISSN: 2171-5068
eISSN: 2171-9845

An intercomparison of satellite burned area maps derived from MODIS, MERIS, SPOT-VEGETATION and ATSR images. An application to the August 2006 Galicia (Spain) forest fires

M. Huesca[1], S. Merino-de-Miguel[2]* and F. Gonzalez-Alonso[3]

[1] *ETSI Montes. Universidad Politécnica de Madrid. Ciudad Universitaria, s/n. 28040 Madrid, Spain*
[2] *EUIT Forestal. Universidad Politécnica de Madrid. Ciudad Universitaria, s/n. 28040 Madrid, Spain*
[3] *Laboratorio de Teledetección. CIFOR-INIA. Ctra. A Coruña, km 7,5. 28040 Madrid, Spain*

Abstract

Aim of study: The following paper presents an inter-comparison of three global products: MCD45A1 (MODIS-MODerate resolution Imaging Spectrometer-Burned Area Product), L3JRC (Terrestrial Ecosystem Monitoring Global Burnt Area Product), and GLOBCARBON Burnt Area Estimate (BAE) Product; and three local products, two of them based on MODIS data and the other one based on MERIS (MEdium Resolution Imaging Spectrometer) data.

Area of study: The study was applied to the Galician forest fires occurred in 2006.

Material and methods: Materials used involved the three already mentioned global products together with two MODIS and one MERIS reflectance images, and MODIS thermal anomalies. The algorithm we used, which is based on the determination of thresholds values on infrared bands, allowed the identification of burned pixels. The determination of such threshold values was based on the maximum spatial correlation between MODIS thermal anomalies, and infrared reflectance values. This methodology was applied to MODIS and MERIS reflectance bands, and to the NBR (Normalized Burn Ratio). Burned area validation was evaluated using burned area polygons as derived from an AWiFS (Advanced Wide Field Sensor) image of 60 m pixel size.

Main results: Best results were reached when using the MERIS infrared bands, followed by the MODIS infrared bands. Worst results were reached when using the MCD45A1 product, which clearly overestimated; and when using the L3JRC product, which clearly underestimated.

Research highlights: Since the efficiency of the performance of the available burned area products is highly variable, much work is needed in terms of comparison among the available sensors, the burned area mapping algorithms and the resulting products.

Key words: forest fires; MODIS; MERIS; MCD45A1; L3JRC; GLOBCARBON-BAE; SPOT-VEGETATION; ATSR.

Introduction

Each year, wildfires affect 3 millions of squared kilometers around the world (Van der Werf *et al.*, 2010). Information on fire activity, which is typically characterized by means of burned area maps, is needed in a rapid, accurate, and cost-effective manner in order to prioritize forest management activities and plan future restoration works (Pyne *et al.*, 1996; González-Alonso *et al.*, 2007). This fact is of particular importance in the Mediterranean basin, where the destruction of the landscape due to fire may amplify the risk of desertification. Besides, both the frequency and intensity of forest fires are expected to increase in the following

* Corresponding author: silvia.merino@upm.es
Received: 30-08-12. Accepted: 26-05-13.

Abbreviations used: ATSR (Along Track Scanning Radiometer); AVHRR (Advanced Very High Resolution Radiometer); AWiFS (Advanced Wide Field Sensor); EOS (Earth Observation System); ESA (European Space Agency); GBA2000 (Global Burnt Area 2000); GLOBCARBON-BAE (GLOBCARBON Burnt Area Estimate Product); L3JRC (Terrestrial Ecosystem Monitoring Global Burnt Area Product); MCD45A1 (MODIS Burned Area Product); MERIS (MEdium Resolution Imaging Spectrometer); MOD09GA (Terra MODIS Surface Reflectance Daily L2G Global 500 m); MOD09GQ (Terra MODIS Surface Reflectance Daily L2G Global 250 m); MODIS (MODerate resolution Imaging Spectrometer); NBR (Normalized Burn Ratio); NDVI (Normalized Difference Vegetation Index); NIR (near-infrared); SPOT (Satellite Pour l'Observation de la Terre), SWIR (short-wave infrared); UTM: (Universal Transverse Mercator).

decades because of the increase of annual and summer temperatures and the reduction of summer rainfall due to the global warming effect (Pausas, 2004; Alcamo *et al.*, 2007). In addition, forest fires release a significant amount of greenhouse gases, particulates, and aerosol emissions into the atmosphere, which in turn significantly increases the anthropogenic CO_2 emissions and the global warming phenomenon itself (Crutzen and Andreae, 1990; Levine, 1991; Van Leeuwen *et al.*, 2010).

The use of remote sensing data may provide temporal and spatial coverage of wildfires without the need for costly and intensive fieldwork. In this sense, one of the most direct and useful information about a forest fire is the mapping of the affected area (Lentile *et al.*, 2006). Traditionally, burned area has been measured using field or airplane surveys in combination with GPS (Global Positioning System) techniques. In general terms, burned area can be estimated using remote sensing techniques in a rapid, economic, and effective way (Lentile *et al.*, 2006), and the results may be directly integrated into a GIS (Geographic Information System). However, in relation to fire, remote sensing techniques and data may be also used in many other applications: fire occurrence and fire patterns (Pereira *et al.*, 2005; Riaño *et al.*, 2007; Ichoku *et al.*, 2008), fire emissions (Palacios-Orueta *et al.*, 2005; Van der Werf *et al.*, 2010), active fire detection (Roy, 1999; Li *et al.*, 2004; Calle *et al.*, 2008), fire and burn severity (De Santis and Chuvieco, 2007; Roldán-Zamarrón *et al.*, 2006), effects of fire on vegetation and soil (Wittenberg *et al.*, 2007), and post-fire vegetation recovery (Riaño *et al.*, 2002, Van Leeuwen *et al.*, 2010).

Satellite-based strategies for burned area mapping, which has been conducted using a wide range of sensors, may use different approaches (Barbosa *et al.*, 1999; Pereira 2003; Lentile *et al.*, 2006). Most of the satellite-based burned area studies rely on variations in pixel reflectance or emittance properties from previous (pre-fire) or surrounding (post-fire) data, by means of either the original bands or some spectral indices. Some studies have also investigated the utility of techniques such time series analysis (Roy *et al.*, 2005), active fire locations (Justice *et al.*, 2002), and hybrid methods (Fraser *et al.*, 2000). These and some other methodologies have been applied profusely during the last decades both at local and regional/global scales. At global scale, there are several initiatives related to burned area mapping that is worth pointing out: the Global Burnt Area 2000 (GBA2000) (Grégoire *et al.*, 2003), the GLOBSCAR (Simon *et al.*, 2004), the GLOBCARBON Burnt Area Estimate (BAE) Product (Plummer *et al.*, 2006), the L3JRC (Terrestrial Ecosystem Monitoring Global Burnt Area Product) (Tansey *et al.*,, 2008) and the MCD45A1 – the MODIS Burned Area Product (Roy *et al.*, 2005, 2008). However, an important effort on validation and comparison of the results should be done since great discrepancies are shown among results (Boschetti *et al.*, 2004a).

One of the most interesting approaches to be considered for burned area mapping is the integration of post-fire reflectance bands or indices together with active fire information. Following this hybrid model Roy (1999), Fraser *et al.* (2000), Al-Rawi *et al.* (2001), and Pu *et al.* (2004) among others, developed different burn scar detection algorithms, that were mainly based on the use of vegetation indices (*e.g.* the NDVI – Normalized Difference Vegetation Index) and thermal anomalies as derived from the AVHRR (Advanced Very High Resolution Radiometer) sensor. More recently, Huesca *et al.* (2008) and Merino-de-Miguel *et al.* (2010, 2011) have developed a series of works in which MODIS post-fire reflectance data is used in combination with MODIS thermal anomalies for burned area mapping in different regions of Spain and South America.

The work presented here aims at the comparison of different burned area maps (either derived from global or local products) and is applied to the Galician (North-West Spain) forest fires occurred in 2006. In particular, we compared three standard or global products: MCD45A1, L3JRC, and GLOBCARBON-BAE Product; and three local products, all calculated using the algorithm developed by Huesca *et al.* (2008), two of them based on MODIS data and the other one based on MERIS data. Validation was carried out by means of a high-spatial resolution burned area map that was derived from an AWiFS (Advanced Wide Field Sensor) image of 60 m pixel size (González-Alonso and Merino-de-Miguel, 2009). Accuracy results were expressed in terms of commission and omission errors in relation to the AWiFS-derived burned area map.

Material and methods

The approach is applied here to Galicia (northwest Spain) where hundreds of forest fires occurred during the first days of August 2006. This region, situated in the northwest of the Iberian Peninsula, just to the north

of Portugal, is one of the most humid parts of Spain. The study area covers 29,681.65 km^2, almost 70 % of which, according to the Third National Forest Inventory (1997-2006), is classified as "forested", with 64% being tree-covered (conifers and eucalyptuses mainly). In this region, woodland fires are usually small but frequent. In fact, Galicia is undoubtedly the region with the greatest concentration of wildfires in Spain. During August 2006, nearly 930 km^2 were almost entirely burned over the course of eight days, producing significant economic losses and severe social upheaval. It is thought that about 90% of the forest fires were caused by people.

Material

Eight sources of data were used for this work: (i) a couple of MODIS post-fire images, (ii) one MERIS post-fire image, (iii) a time series of MODIS active fires, (iv) the MODIS Burned Area Product (MCD45A1) for the study area and period of interest, (v) the L3JRC Burned Area Product for the study area and period of interest, (vi) the GLOBCARBON-BAE product, (vii) the AWiFS-derived burned area perimeters for validation purposes, and (viii) administrative maps.

We used two post-fire MODIS images that were downloaded free of charge from the EOS (Earth Observation System) Data Gateway. They consisted of atmospherically corrected surface reflectance daily products: (i) at 250 m spatial resolution [MOD09GQ – Terra MODIS Surface Reflectance Daily L2G Global 250 m, with 2 bands: red and near-infrared (NIR)], and (ii) at 500 m spatial resolution [MOD09GA – Terra MODIS Surface Reflectance Daily L2G Global 500 m, with 7 bands: blue, green, red, NIR and three bands in the shortwave-infrared (SWIR)]. Both images were acquired on the 21st of August, 2006 and were cloud-free. MERIS is a multi-spectral sensor with fifteen programmable narrow bands in the visible and NIR regions of the spectrum. We used one MERIS post-fire image that was acquired on the 22nd of August, 2006 in the Full Resolution mode (300m pixel size).

The MODIS time series of active fires (NASA / University of Maryland, 2002), that were provided free of charge by the University of Maryland, consisted of a set of shape files with one record per active fire. Information related to each active fire included: location (latitude and longitude), date, time, confidence level, and satellite involved. The MODIS active fire locations covered the study area and period of interest (1st-20th August, 2006). A general description of the MODIS fire products can be found in Justice *et al.* (2002). A detailed description of the MODIS active fire detection algorithm (version 4) can be found in Giglio *et al.* (2003).

For comparison and evaluation purposes, we used three global burned area datasets: the MCD45A1 (MODIS Terra + Aqua Burned Area Monthly L3 Global 500 m), the L3JRC (Global, daily, SPOT VEGETATION-derived Burned Area Product, 1 km), and the GLOBCARBON-BAE Product (Global, Monthly 1 km based on SPOT-VGT and ATSR images). The MCD45A1 product (Roy *et al.* 2005, 2008) was downloaded from the EOS Data Gateway, while the L3JRC product (Tansey *et al.,* 2008) was downloaded from the Global Environment Monitoring Website, both of which were free of charge.

The GLOBCARBON-BAE Product, which consists of three layers as a result of combining three algorithms, detects the appearance of new burned areas from month to month, and is available for the period 1998-2007 (Plummer *et al.*, 2006). The GLOBCARBON-BAE product we used was whenever two out of the three algorithms agreed.

For validation purposes, we used a high spatial resolution AWiFS-derived burned area map that was compared to each of the burned area products. AWiFS, onboard Resourcesat-1 satellite, is a unique sensor that provides data with a spatial resolution of 56 m at 5-day intervals in four spectral bands (green, red, NIR, and SWIR). Fig. 1 shows the AWiFS-derived burned area map.

Methods

Fig. 2 summarizes the methodology followed in this work. On the one hand, we processed the MODIS and MERIS datasets based on the algorithm developed by Huesca *et al.* (2008). On the other hand, we also prepared the three already mentioned global burned area products for further analysis. All the processing of the data was carried out using ENVI 4.5 and ArcGIS 9.3.1 software packages. The coordinate system we used was the UTM-Zone 30-WGS-84.

The algorithm developed by Huesca *et al.* (2008), which aims at the determination of thresholds values on infrared bands, is based on the maximum spatial correlation between MODIS active fire influence area, and post-fire infrared reflectance values. MODIS active fires, which are expressed as point locations, were

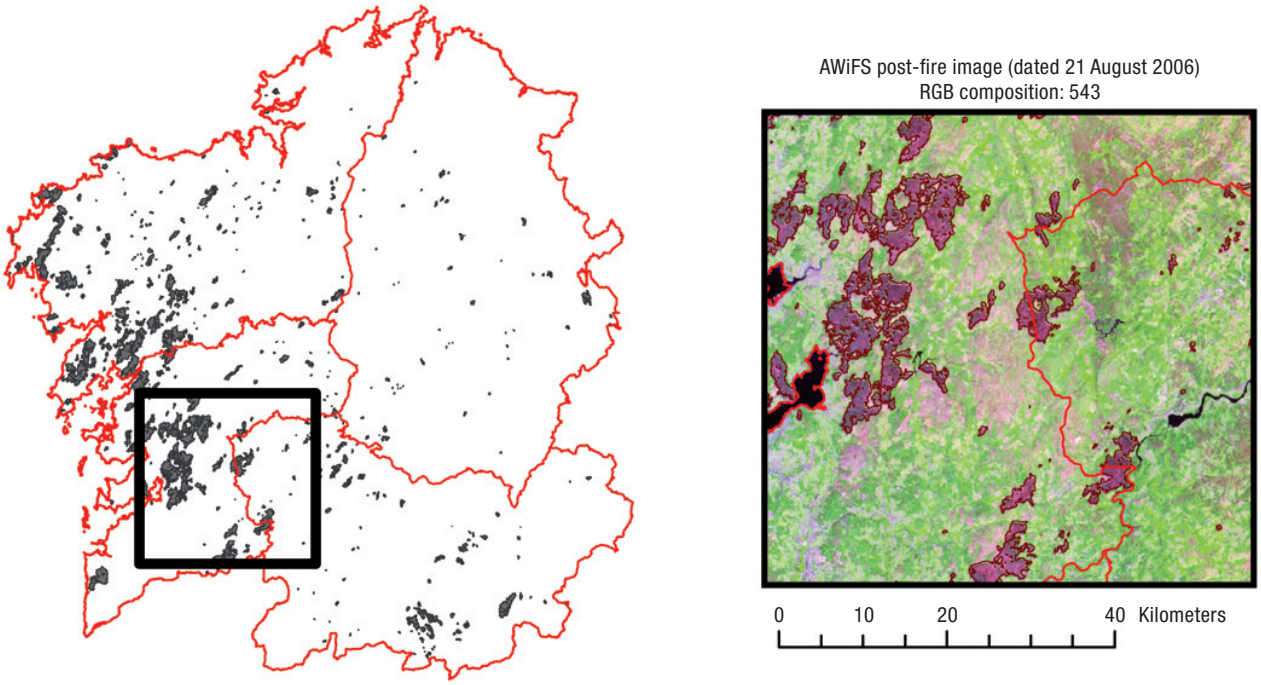

Figure 1. 60 m spatial resolution AWiFS-derived burned area map (21st August, 2006).

assumed to be located inside an area of 1 km^2 (Salmon *et al.*, 2003), the so-called influence area. In this sense, we generated a buffer layer of influence areas as closest in size as possible to 1 km^2, what meant using (i) 16 pixels of 250 m in the case of the MOD09GQ product, (ii) 4 pixels of 500 m for the MOD09GA product, and (iii) 9 pixels of 300 m for the MERIS image.

In this work, the Huesca *et al.* (2008) methodology was applied: (i) to the MOD09GQ NIR band, (ii) to the MOD09GA NBR index, and (iii) to one of the MERIS reflectance NIR bands. The NBR (Key and Benson, 1999) is a spectral index that integrates NIR and SWIR bands, both of which register the strongest responses, albeit in opposite ways, to burning (Lentile *et al.*, 2006, Roldán-Zamarrón *et al.*, 2006). The NBR was estimated using the following equation:

$$NBR = (\rho_{SWIR} - \rho_{NIR})/(\rho_{SWIR} + \rho_{NIR}) \qquad [1]$$

where, ρ_{SWIR} and ρ_{NIR} are the SWIR and NIR pixel reflectance values, respectively. Using equation [1], the NBR was calculated using bands 2 (NIR) and 7 (SWIR) of the MOD09GA product. MERIS images have several bands at NIR wavelengths. In this case, and in order to compare the results between MODIS and MERIS, we selected the MERIS NIR band that was closest to the MODIS band 2 wavelength, what resulted in the selection of the MERIS band centered at 864 nm.

In this work, we looked for the highest spatial correlation between MODIS active fire influence area and a set of binary MODIS-NIR (MOD09GQ), MODIS-NBR (MOD09GA), and MERIS-NIR images. These binary images were derived using a subset of threshold values. Spatial coincidence was measured by means of the correlation coefficient. The application of the best threshold value in each case resulted in three burned-unburned images that assured the greatest consistency between active fires information and post-fire reflectance-based data. These burned-unburned images-were converted into vector format. At this point, and based on previous results (Huesca *et al.*, 2008; González-Alonso and Merino-de-Miguel 2009), we removed any polygon that was situated far away from an active fire, at a distance higher than 564.18 m, in an attempt to reduce the commission error.

The processing of the three global burned area products consisted on the re-projection onto a UTM-Zone 30 -WGS-84 coordinate system, together with a spatial and temporal subset according to the study area (Galicia) and period of interest (1st-20th August, 2006).

Validation of the results (either local or global burned area products) was performed using the AWiFS-derived burned area map (our ground-truth) by means of cross-tabulation. The validation process served to verify the quality of the different burned area maps

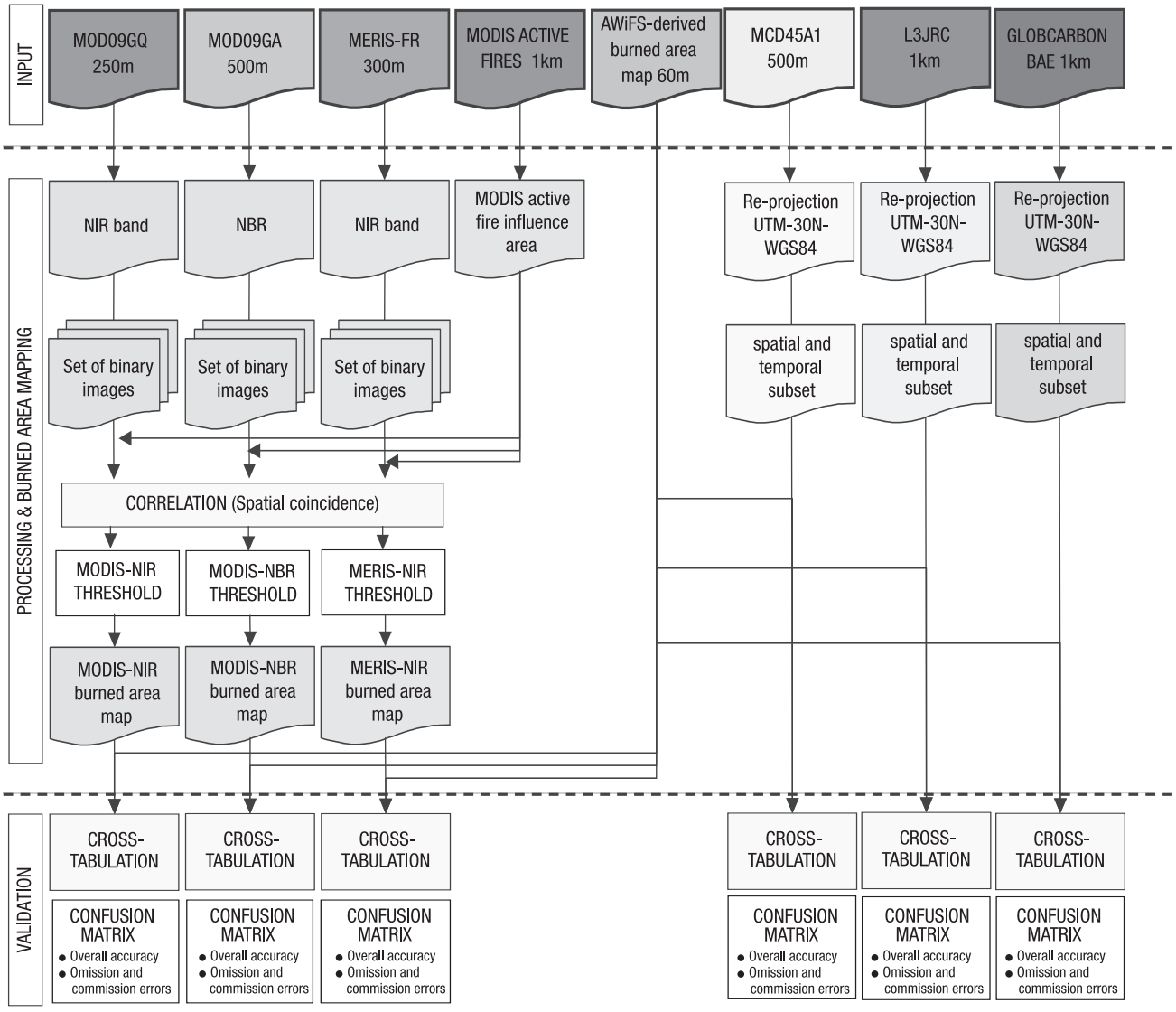

Figure 2. Methodology flow followed in this work.

and to rank them, identifying the gains and weaknesses of any of the evaluated products. The validation data (or ground-truth) represent the reality (*e.g.,* free from errors), and thus, they serve as a reference to measure the accuracy of the classification process (Boschetti *et al.*, 2004b). One of the most common means of validation in remote sensing is using data derived from higher spatial resolution images, as we did in this case. The results of the cross-tabulation between datasets (two by two) were summarized in confusion matrices (Stehman, 1997) that were used to extract two parameters: (i) the overall accuracy, and (ii) the omission and commission errors for the burned class.

Results

Local burned area products resulted from the selection of the appropriate threshold values and the removal of those polygons not containing at least one active fire inside or within a distance of less than 564.18 m. In all the cases, the percentage of coincidence rises from low NIR values to a maximum value and them drops drastically. The NIR value at which we found the highest spatial coincidence between active fire influence area and post-fire data was selected as the threshold value that allowed the best discrimination between burned and un-burned pixels. Such threshold values were: (i) 14% for the MODIS-NIR (MOD09GQ-band 2), (ii)

Table 1. Results form the cross-tabulation between any of the burned area maps and our ground truth

	Burned area (km^2)	Overall accuracy (%)	Error omission (%)	Error commission (%)
MODIS-NIR	799.58	65.37	34.62	20.37
MODIS-NBR	679.00	51.17	48.83	21.64
MERIS-NIR	794.24	65.72	34.28	18.45
MCD45A1	1,542.75	79.21	20.79	86.21
L3JRC	426.49	28.30	71.70	17.43
GLOBCARBON-BAE	843.95	53.89	46.11	36.61
AWiFS-based burned area map (ground truth)	932.61			

0.07 for the MODIS-NBR (MOD09GA-NBR), and (iii) 13% for the MERIS-NIR (centered at 864 nm) band.

Table 1 shows the results from the cross-tabulation between the different burned area products and our ground truth (the AWiFS-derived burned area map). The cross-tabulation analysis was performed using all the data in polygon-vector format. As a result of the cross-tabulation we calculated the overall accuracy and both the commission and omission errors. Fig. 3 shows the spatial distribution of coincident areas (overall accuracy) and both the commission and omission errors for two products, one local and one global product.

As shown in Table 1, results for the MODIS-NIR and the MERIS-NIR bands are very close in terms of burned area, overall accuracy, and omission and commission errors. The results for the MODIS-NBR band are slightly worse, especially in terms of overall accuracy and error of omission. However, the worst results undoubtedly corresponded to the global burned area products (MCD45A1, L3JRC, and GLOBCARBON-BAE). The best result in terms of overall accuracy corresponded to the MODIS burned area product (MCD45A1). However, this is no such a good result if we check for the error of commission. On the other hand, the L3JRC presented a very low overall accuracy together with a very high error of omission. Results for the GLOBCARBON-BAE product were intermediate between the other two global products.

Discussion

One of the most interesting applications of the remote sensing data in the study of wildfires is the burned area mapping (Lentile *et al.*, 2006; Loboda *et al.*, 2007). The mapping of the affected area can be generated using diverse methods and technologies and it is now globally available thanks to some large-scale products. Proper assessment of these global products is complex and costly but it is nowadays becoming increasingly important (Chuvieco *et al.*, 2008; Roy and Boschetti, 2009). It is a fact that only these products may provide information about burned areas at global scale but also that their accuracy is highly dependent on the cover type, fire occurrence and fire scar size (Loboda *et al.*, 2007), and on the study region (Giglio *et al.*, 2010). Besides, since the efficiency of the performance of such global products may also differ in different ecosystems (Loboda *et al.*, 2007) much work is needed in terms of comparison among the available sensors, the burned area mapping algorithms and the resulting products. The present work, along with previous studies that compared global fire products at different scales (Boschetti *et al.*, 2004a; Laris, 2005; Silva Cardozo *et al.*, 2012), suggests the need of a better validation of these products, especially in the Iberian Peninsula where the discrepancies found in the present work agree with the studies of Bastarrika *et al.* (2011) and Padilla and Chuvieco (2009).

The present work compares the algorithm developed by Huesca *et al.* (2008) using different sensors (MODIS and MERIS) and approaches. The results showed no much difference between one and the other. Higher and more significant differences appeared when compared the different local burned area products to the three available global burned area maps (MCD45A1, L3JRC, and GLOBCARBON-BAE), as also shown by other authors (Bastarrika *et al.*, 2011). As expected, these three global products showed similar burn scars patterns both among them (Giglio *et al.*,

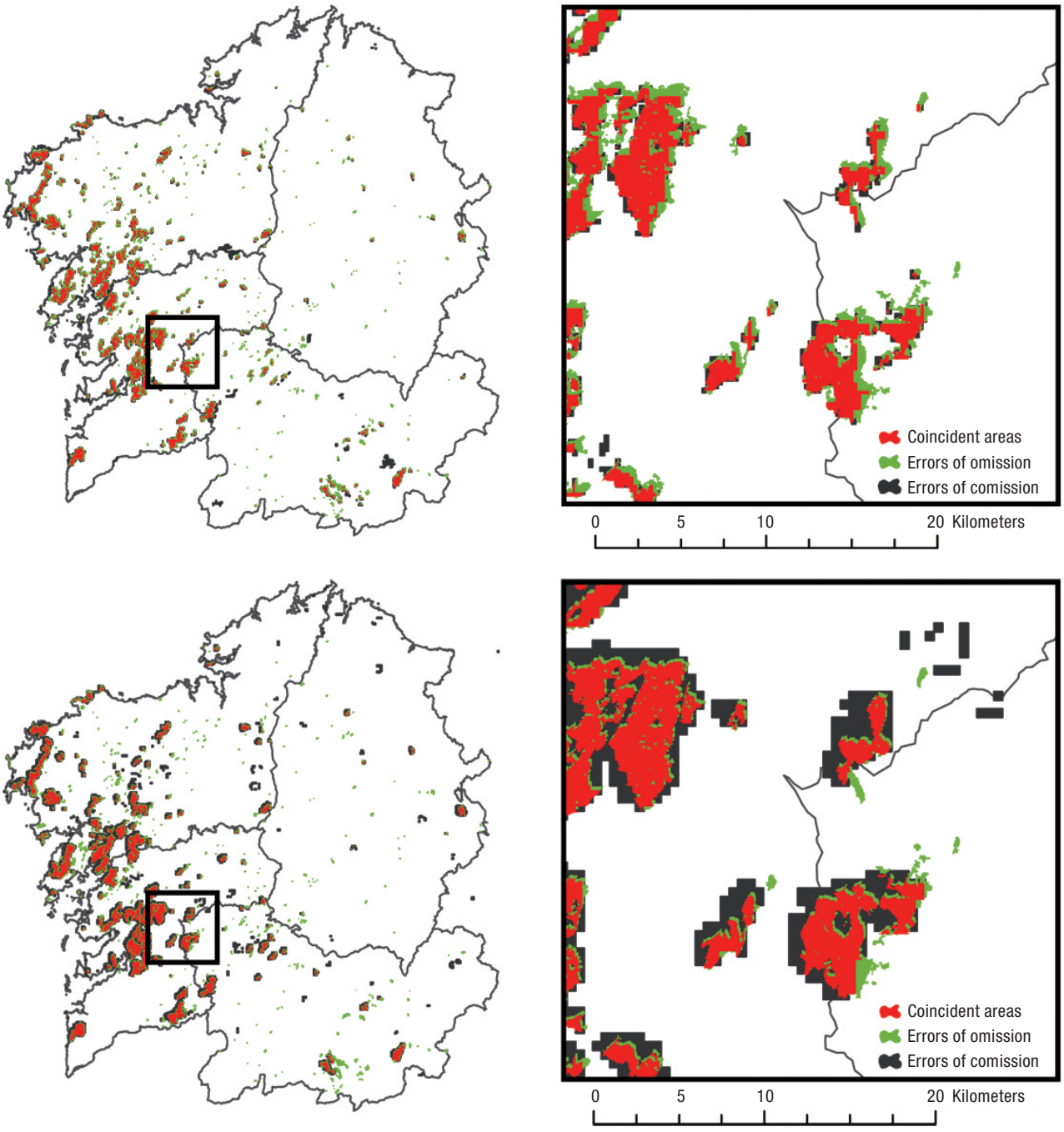

Figure 3. Top image: MERIS-NIR-based against AWiFS-based burned area map. Bottom image: MCD45A1 against AWiFS-based burned area map. Legend: in red: coincident areas, in green: errors of omission and in black: errors of commission.

2010) and when compared to our products. On the one hand, considering the overall accuracy of the burned area and without taking into account commission or omission errors, the most accurate product was the MCD45A1 one, as also shown by Anaya and Chuvieco (2012), followed by the GLOBCARBON-BAE, and finally by the L3JRC product. Same results were also found by Roy and Boschetti (2009), supporting the idea of the need of a more consistent global fire product validation. On the other hand, considering the total amount of burned area and its geographical accuracy important differences arose among them, especially in

the case of the MODIS burned area product (MCD45A1), which clearly overestimated the affected area (high commission error, see table 1) and in the case of the L3JRC product, which clearly underestimated the affected area (high omission error, see Table 1). On contrary, Roy and Boschetti (2009) found, in their validation of the three global products, lower errors of commission than omission. Similar results were revealed by Silva Cardozo *et al.* (2012) in relation to the validation of the MCD45A1 product in the Amazon region, where high or very high omission errors were found.

As mentioned before, we found that the MCD45A1 product clearly overestimated the total burned area while in Bastarrika *et al.* (2011), in a study carried out in Mediterranean ecosystems; the same variable was noticeably underestimated. These discrepancies may be explained by the fact that Galician fire scars were mainly located in the Atlantic region rather than in the Mediterranean region (González-Alonso and Merino de Miguel, 2009). Anaya and Chuvieco (2012) also found that the MODIS burned area product underestimated the burned area for the Orinoco River basin. According to our results, burned area estimated from the L3JRC product is clearly lower that the other products. Similar results were found by Anaya and Chuvieco (2010, 2012) while in other studies (Chang and Song, 2009) the burned area was overestimated. Opposite results were also found by Giglio *et al.* (2010) in which study L3JRC product mapped a burned area many times larger than the MCD45A1 product in seven regions worldwide including Europe. Concerning the GLOBCARBON-BAE product, Anaya and Chuvieco (2012) found that this product tended to underestimate the burned area.

Global products may provide estimates of the total burned area at large scales. These estimations are critical from both an ecological and management point of view (Chuvieco *et al.*, 2008) and for feeding fire emissions and climatic models (Giglio *et al.*, 2010). However, more site-dependant algorithms are necessary in order to improve the burned area mapping accuracy. This is not a simple task since most of the available regional products have been specifically designed for a given ecosystem, dropping their mapping accuracy when applied to other biomes (Loboda *et al.*, 2007). This paper evidences the importance of developing regionally-adaptable algorithms which, in combination with the global fire products, may improve the accuracy of the estimates. This kind of studies may also be useful for the customization and regionalization of the available global burned area products, or for the development of new indices and methodologies. In this sense, it is necessary the comparison among same products in different regions and land cover types but also it is necessary a comparison with independent ground-truth or independent reference data (Roy and Boschetti, 2009) in order to solve the problems associated with the commission and omission errors (Boschetti *et al.*, 2004b).

The local burned area algorithms developed in this paper present a straightforward and repeatable approach which can be easily used in other biomes by simply look for the appropriate threshold value. Besides, our algorithm is fully automated, it does not rely on an analyst's opinion therefore eliminating subjectivity of the mapping process, and it is based on free data available on the Internet. However, the presented results make it difficult to draw conclusions about the reliability of our algorithm performance over other regions in the Iberian Peninsula and outside the Iberian Peninsula. As weak points, the algorithms tended to produce omission errors that were higher than the corresponding commission errors. This fact may be due to the missing active fire locations between Terra-MODIS successive images, a situation that may cause an infra-estimation of the burned area (Giglio *et al.*, 2003).

Conclusions

This article presents the results of applying several local burned area algorithms together with global burned area maps, and compares all the results in relation to a high spatial resolution burned area map (our ground-truth). The local burned area maps produced very accurate results in any case (either using MODIS or MERIS data). The needed information (reflectance and active fire data) is available free of charge through the Internet, and the processing of the data is extremely simple. On the other hand, the global burned area products tended to product worse results, in some cases because the product tended to overestimate the affected area (MCD45A1) or because the product tended to underestimate the affected area (L3JRC).

Acknowledgements

The authors would like to thank the NASA EOS Data Gateway and University of Maryland for supplying Terra/Aqua MODIS products. We also thank ESA for

supplying MERIS data, and the GLOBCARBON-BAE products as well as Global Environment Monitoring for providing L3JRC products. The participation of Dr. Federico González-Alonso in this work has been done in the context of development of the project ESA-ECV-CCI-Fire.

References

Alcamo J, Moreno J, Nováky B, Bindi M, Corobov R, Devoy R *et al.,* 2007. Climate change 2007, impacts, adaptation and vulnerability. Europe. Contribution of working group II to the fourth assessment report of the intergovernmental panel on climate change. Cambridge University Press, Cambridge. pp: 541-580.

Al-Rawi K, Casanova J, Romo A, 2001. IFEMS: a new approach for monitoring wildfire evolution with NOAA-AVHRR imagery. Int J Remote Sens 22: 2033-2042.

Anaya-Acevedo J, Chuvieco-Salinero E, 2010. Validación para Colombia de la estimación de área quemada del producto L3JRC en el periodo 2001-2007. Actual Biol 32: 29-40.

Anaya JA, Chuvieco E, 2012. Accuracy assessment of burned area products in the Orinoco basin. Photogramm Eng Rem S 78: 53-60.

Barbosa PM, Grégoire JM, Pereira JMC, 1999. An algorithm for extracting burned areas from time series of AVHRR GAC data applied at a continental scale. Remote Sens Environ 69: 253-263.

Bastarrika A, Chuvieco E, Martín MP, 2011. Automatic burned land mapping from MODISTime series images: assessment in Mediterranean ecosystems. IEEE T Geosci Remote 49, 3401-3413.

Boschetti L, Eva H, Brivio PA, Gregoire JM, 2004a. Lessons to be learned from the comparison of three satellite-derived biomass burning products. Geophys Res Lett 31: L21501.

Boschetti L, Flasse SP, Brivio PA, 2004b. Analysis of the conflict between omission and commission in low spatial resolution dichotomic thematic products: the Pareto boundary. Remote Sens Environ 91: 280-292.

Calle A, González-Alonso F, Merino-de-Miguel S, 2008. Validation of active forest fires detected by MSG-SEVIRI by means of MODIS hot spots and AWiFS images. Int J Remote Sens 29: 3407-3415.

Chang D, Song Y, 2009. Comparison of L3JRC and MODIS global burned area products from 2000 to 2007. J Geophys Res 114, D16106.

Chuvieco E, Opazo S, Sione W, Valle H, Anaya J, Di Bella C, Cruz I, Manzo L, López G, Mari N, González-Alonso F, Morelli F, Setzer A, Csiszar I, Kanpandegi JA, Bastarrika A, Libonati R, 2008. Global burned-land estimation in Latin America using MODIS composite data. Ecol Appl 18: 64-79.

Crutzen PJ, Andreae MO, 1990. Biomass burning in the tropics: impact on atmospheric chemistry and biogeochemical cycles. Science 250: 1669-1678.

De Santis A, Chuvieco E, 2007. Burn severity estimation from remotely sensed data: performance of simulation *versus* empirical models. Remote Sens Environ 108: 422-435.

Fraser R, Li Z, Cihlar J, 2000. Hotspot and NDVI differencing synergy (HANDS): a new technique for burned area mapping over boreal forest. Remote Sens Environ 74: 362-376.

Giglio L, Descloitres J, Justice CO, Kaufman YJ, 2003. An enhanced contextual fire detection algorithm for MODIS. Remote Sens Environ 87: 273-282.

Giglio L, Randerson JT, Van der Werf GR, Kasibhatla PS, Collatz GJ, Morton DC, DeFries RS, 2010. Assessing variability and long-term trends in burned area by merging multiple satellite fire products. Biogeosciences 7: 1171-1186.

González-Alonso F, Merino-de-Miguel S, 2009. Integration of AWiFS and MODIS active fire data for burn mapping at regional level using the Burned Area Synergic Algorithm (BASA). Int J Wildland Fire 18: 404-414.

González-Alonso F, Merino-De-Miguel S, Roldán-Zamarrón A, García-Gigorro S, Cuevas J, 2007. MERIS Full Resolution data for mapping level-of-damage caused by forest fires: the Valencia de Alcántara event in August 2003. Int J Remote Sens 28: 797-809.

Grégoire JM, Tansey K, Silva J, 2003. The GBA2000 initiative: developing a global burnt area database from SPOT-VEGETATION imagery. Int J Remote Sens 24: 1369-1376.

Huesca M, González-Alonso F, Cuevas J, Merino-de-Miguel S, 2008. Estimación de la superficie quemada en los incendios forestales de Canarias en 2007 utilizando sinérgicamente imágenes MODIS y anomalías térmicas. Investigación agraria. Sistemas y recursos forestales 17: 308-316.

Ichoku C, Giglio L, Wooster MJ, Remer LA, 2008. Global characterization of biomass-burning patterns using satellite measurements of fire radiative energy. Remote Sens Environ 112: 2950-2962.

Justice C, Giglio L, Korontzi S, Owens J, Morisette J, Roy D *et al., 2*002. The MODIS fire products. Remote Sens Environ 83: 244-262.

Key CH, Benson NC, 1999. Measuring and remote sensing of burn severity: the CBI and NBR. In: Proceedings Joint Fire Science Conference and Workshop (Neuenschwander LF, Ryan KC, eds). Vol. II, Boise, ID, 15-17 June 1999. University of Idaho and International Association of Wildland Fire. 284 pp.

Laris PS, 2005. Spatiotemporal problems with detecting and mapping mosaic fire regimes with coarse-resolution satellite data in savanna environments. Remote Sens Environ 99: 412-424.

Lentile LB, Holden ZA, Smith AMS, Falkowski MJ, Hudak AT, Morgan P *et al., 2*006. Remote sensing techniques to assess active fire characteristics and post-fire effects. Int J Wildland Fire 15: 319-345.

Levine JS, 1991. Global biomass burning: atmospheric, climatic, and biospheric implications. The MIT Press. Cambridge, USA.

Li RR, Kaufman YJ, Hao WM, Salmon JM, Gao BC, 2004. A technique for detecting burn scars using MODIS data.

IEEE Transactions on Geoscience and Remote Sensing 42: 1300-1308.

Loboda T, O'Neal K, Csiszar I, 2007. Regionally adaptable dNBR-based algorithm for burned area mapping from MODIS data. Remote Sens Environ 109: 429-442.

Merino-de-Miguel S, González-Alonso F, Huesca M, Armenteras D, Franco C, 2011. MODIS reflectance and active fire data for burn mapping in Colombia. Earth Interact 15: 1-17.

Merino-de-Miguel S, Huesca M, González-Alonso F, 2010. MODIS reflectance and active fire data for burn mapping and assessment at regional level. Ecol Model 221: 67-74.

NASA/University of Maryland 2002 MODIS Hotspot/Active Fire Detections. Data set. MODIS Rapid Response Project, NASA/GSFC [producer], University of Maryland, Fire Information for Resource Management System [distributors]. Available on-line [http://maps.geog.umd.edu].

Padilla M, Chuvieco E, 2009. Validación de productos globales de área quemada en la Península Ibérica. Revista de Teledetección 31, 69-79.

Palacios-Orueta A, Chuvieco E, Parra A, Carmona-Moreno C, 2005. Biomass burning emissions: a review of models using remote-sensing data. Environ Monit Assess 104: 189-209.

Pausas JG, 2004. Changes in fire and climate in the eastern Iberian Peninsula (Mediterranean basin). Clim Change 63: 337-350.

Pereira JMC, 2003. Remote sensing of burned areas in tropical savannas. Int J Wildland Fire 12: 259-270.

Pereira MG, Trigo RM, da Camara CC, Pereira J, Leite SM, 2005. Synoptic patterns associated with large summer forest fires in Portugal. Agric For Meteorol 129: 11-25.

Plummer S, Arino O, Simon M, Steffen W, 2006. Establishing a earth observation product service for the terrestrial carbon community: the GLOBCARBON initiative. Mitigation Adapt Strat Global Change 11: 97-111.

Pu R, Gong P, Li Z, Scarborough J, 2004. A dynamic algorithm for wildfire mapping with NOAA/AVHRR data. Int J Wildland Fire 13: 275-285.

Pyne S, Andrews P, Laven R, 1996. Introduction to wildland fire. Final report MMF Practices-3015, Canada.

Riaño D, Moreno Ruiz J, Isidoro D, Ustin S, 2007. Global spatial patterns and temporal trends of burned area between 1981 and 2000 using NOAA-NASA Pathfinder. Global Change Biol 13: 40-50.

Riaño D, Chuvieco E, Ustin S, Zomer R, Dennison P, Roberts D, Salas J, 2002. Assessment of vegetation regeneration after fire through multitemporal analysis of AVIRIS images in the Santa Monica Mountains. Remote Sens Environ 79: 60-71.

Roldán-Zamarrón A, Merino-de-Miguel S, González-Alonso F, García-Gigorro S, Cuevas J, 2006. Minas de Riotinto (south Spain) forest fire: burned area assessment and fire severity mapping using Landsat 5-TM, Envisat-MERIS, and Terra-MODIS postfire images. Journal of geophysical research 111: G04S11.

Roy D, 1999. Multi-temporal active-fire based burn scar detection algorithm. Int J Remote Sens 20: 1031-1038.

Roy D, Jin Y, Lewis P, Justice C, 2005. Prototyping a global algorithm for systematic fire-affected area mapping using MODIS time series data. Remote Sens Environ 97: 137-162.

Roy D, Boschetti L, Justice C, Ju J, 2008. The collection 5 MODIS burned area product – Global evaluation by comparison with the MODIS active fire product. Remote Sens Environ 112: 3690-3707.

Roy D, Boschetti L, 2009. Southern Africa validation of the MODIS, L3JRC and GlobCarbon Burned-area products. IEEE T Geosci Remote 47: 1032-1044.

Salmon J, Hao W, Miller M, Nordgren B, Kaufman Y, Li R, 2003. Validation of two MODIS single-scene fire products for mapping burned area: hot spots and NIR spectral test burn scars. In: 4th International Workshop on Remote Sensing and GIS – Applications to Forest Fire Management: Innovative concepts and methods in fire danger estimation: 197-202.

Silva Cardozo F, Pereira G, Edemir Shimabukuro Y, Caria Moraes E, 2012. Validation of MODIS MCD45A1 Product to identify burned areas in Acre State – Amazon Forest. IGARSS 2012: 6741-6744.

Simon M, Plummer S, Fierens F, Hoelzemann J, Arino O, 2004. Burnt area detection at global scale using ATSR-2: the GLOBSCAR products and their qualification. Journal of Geophysical Research 109: D14S02.

Stehman SV, 1997. Selecting and interpreting measures of thematic classification accuracy. Remote Sens Environ 62: 77-89.

Tansey K, Grégoire JM, Defourny P, Leigh R, Pekel JF, Van Bogaert E, Bartholomé E, 2008. A new, global, multi-annual (2000-2007) burnt area product at 1 km resolution. Geophys Res Let 35: L01401.

Van der Werf GR, Randerson JT, Giglio L, Collatz G, Mu M, Kasibhatla PS *et al., 2*010. Global fire emissions and the contribution of deforestation, savanna, forest, agricultural, and peat fires (1997-2009). Atmos Chem Phys 10: 11707-11735.

Van Leeuwen WJD, Casady GM, Neary DG, Bautista S, Alloza JA, Carmel Y *et al., 2*010. Monitoring post-wildfire vegetation response with remotely sensed time-series data in Spain, USA and Israel. Int J Wildland Fire 19: 75-93.

Wittenberg L, Malkinson D, Beeri O, Halutzy A, Tesler N, 2007. Spatial and temporal patterns of vegetation recovery following sequences of forest fires in a Mediterranean landscape, Mt. Carmel Israel. Catena 71: 76-83.